0273-2289/02/98-100/1075/$14.25

Effect of Bubble Size on Foam Fractionation of Ovalbumin

Liping Du, Aleš Prokop, and Robert D. Tanner*

Chemical Engineering Department, Vanderbilt University, Nashville, TN 37235,
E-mail: Rtanner@vuse.vanderbilt.edu

Abstract

The bubble size distribution and void fraction (ε_g) (at two bulk liquid pool positions below the bulk liquid–foam interface and one lower foam phase position) in a continuous foam fractionation column containing ovalbumin were obtained using a photoelectric capillary probe. The bubble size and ε_g data were gathered for different operating conditions (including the changes in the superficial gas velocity and feed flow rate) at a feed solution of pH 6.5 and used to calculate the specific area, a, of the bubbles. Thus, local enrichment (ER_l), values of ovalbumin could be estimated and compared with directly obtained experimental results. The ER_l results were also correlated with the bubble size and ε_g to understand better the concentration mechanisms of foam fractionation. The high ER_l in the lower foam phase was largely attributable to the abrupt increase in ε_g (from 0.25 to 0.75), or the a (from about 12 to 25 cm^2/cm^3) from the bulk liquid to the foam phase. These changes correspond with enhanced gravity drainage. With an increase in the superficial gas velocity, the bubble size increased and the a decreased in both the bulk liquid and lower foam phases, resulting in a decrease in the local experimentally determined enrichments at high superficial gas velocities. At intermediate feed flow rates, the bubble size reached the maximum. The ε_g and a, on the other hand, were the largest for the largest feed flow rate. The ER_l in the lower foam phase was maximized at the lowest feed flow rate. It follows, therefore, that a alone is not sufficient to determine the magnitude of the ER_l in the foam phase.

Index Entries: Bubble size; void fraction; foam fractionation; ovalbumin.

Introduction

In a foam fractionation process, bubbles are the carriers of surface-active solutes such as proteins. Bubble size is expected to influence the

*Author to whom all correspondence and reprint requests should be addressed.

performance of the foam fractionation process since it not only determines the interfacial area where adsorption of protein occurs, but also affects the drainage and coalescence in the foam phase. Rand and Kraynik *(1)* have found that the stability of foam is enhanced with smaller bubbles owing to a decrease in drainage. Sarma and Khilar *(2)* reported that a uniform bubble size distribution favored stable foams.

Bubble size in a foam fractionation column (foam is generated by sparging) is determined by the type of sparger used. Bhattacharya et al. *(3)* employed a sparger disk (pore size: 100 μm) and measured the bubble size by photography. However, they did not report the details of their results. They concluded that an increased bubble size improved the enrichment. Brown et al. *(4)* used both the flat plate (pore size: 0.1 mm) and the sintered (pore size 16–40 μm) spargers in the foam fractionation of β-casein. Their results showed the bubble sizes produced by the flat plate sparger were always greater than those produced by the sintered glass sparger. They hypothesized that the bubble size significantly influenced the protein concentration in the foam as well as foamate flow rate and, hence, enrichment. They found also that the larger bubble size favored higher enrichments but did not significantly affect the separation ratio. Brown et al. *(5)*, Uraizee and Narsimhan *(6)*, and Bhattacharya et al. *(3)* all found that smaller bubbles promoted protein recovery. This enhanced recovery is the result of the increased interfacial area and greater liquid holdup in the foam.

Wong et al. *(7)* used a glass frit with a pore size range of 15–40 μm in a foam fractionation process of bovine serum albumin (BSA) and presented their bubble size distribution measurement (determined by photography) results for different liquid pool and foam positions. It was shown that the bubble size distributions in both the liquid pool and the foam phase were broad (ranging from 0 to 5.0 mm) and generally could be represented by a log normal distribution. The average bubble diameter (Sauter mean, d_{32}) increased for high airflow rates, and this effect was most significant in the foam phase.

In Brown et al.'s *(5)* continuous foam fractionation experiments, fritted glass disks were used with a small pore size (4–10 μm). The bubble size was measured using photography. They found that the number average bubble radius in the foam phase just above the bulk liquid-foam interface increased as the feed concentration and the gas flow rate decreased, but these effects were not significant. For instance, when the feed concentration decreased from 0.2 to 0.01% wt, the number average bubble radius increased from 0.16 to 0.21 mm. The radius increased from 0.205 to 0.215 mm as the gas flow rate decreased from 0.1 to 0.05 cm/s. They concluded that the larger bubbles led to a decrease in the liquid holdup and BSA enrichment. The bubble size distributions that they measured were broad, and the area average size was larger than the number average size. They suggested that the larger bubbles had a greater effect on the drainage and, hence, the liquid holdup, while the smaller bubbles had a greater effect on the surface area. More coalescence along the foam height was

observed, which is thought to contribute to the increase in bubble size. Coalescence acts as internal reflux, decreasing the surface area (by increasing the bubble size) and broadening the bubble size distribution. Large bubbles tend to hasten the rate of liquid drainage and provide a much smaller interfacial area, whereas smaller bubbles yield larger interfacial area at the cost of a much slower drainage rate. Brown et al.'s *(5)* model theoretically predicted that the overall effect of the bubble size distribution was detrimental to both enrichment and recovery.

Uraizee and Narsimhan *(6)* employed capillaries to generate uniform bubbles. They investigated the effect of different capillary diameters (0.076–0.15 mm) on the bubble sizes in a foam fractionation column. The BSA enrichment was found to be higher for larger bubble sizes generated by larger capillary diameters, but the increase was small.

Discernment of the bubble size distribution in foam is essential for an improved understanding of the foam properties and the stability of those properties *(8)*. Our study used a photoelectric capillary probe to measure the bubble size distributions in a continuous foam fractionation column containing ovalbumin. Experimentally measured results of the bubble size and void fraction are presented herein. The specific areas of the bubbles are calculated using these measurements. The local enrichments are calculated and compared with the direct experimental results.

Materials and Methods

Figure 1 shows the continuous foam fractionation and bubble size measurement set-up *(9)*. Continuous foam fractionation experiments were carried out in a glass column (14 cm id, 50 cm length). Compressed air was introduced into the column through a porous sparger (14 cm diameter, pore size of 40–60 μm) mounted flush to the glass wall at the bottom of the column. The airflow rate was adjusted at the rotameter (King Instrument). To minimize the loss of water from the bulk liquid to the air effluent stream, air was passed through a humidifier before it entered the column. The inlet end of the capillary probe was submerged vertically in the bulk liquid phase (referred to as –12 cm and –1 cm) or the foam phase (referred to as +1 cm and +21 cm) in order to measure the local bubble size distribution and the void fraction, ε_g. Gas-liquid dispersion samples were withdrawn through the measuring capillary by applying a vacuum to the capillary outlet. While the bubble size distribution and ε_g were measured online, the effluent gas-liquid dispersion was collected as a liquid (foamate) in a buffer bottle, and its concentration was subsequently analyzed using the Bradford Coomassie Blue method *(10)*. The input feed flow rate was controlled by changing the speed of the liquid pump (Masterflex, cat. no. 755320; Cole Parmer). The liquid pool level was kept constant at 28 cm by adjusting the continuous output residue solution flow rate to equal the difference between the feed flow rate and the net liquid flow rate that was carried from the foam phase into the top foamate collector.

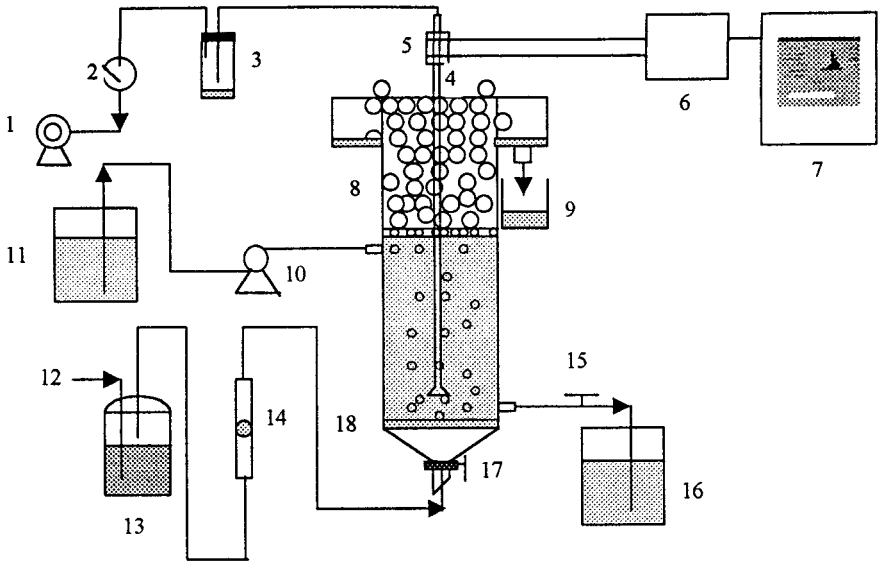

Fig. 1. Experimental setup of continuous foam fractionation process and bubble size measurement apparatus. 1, Precision vacuum pump; 2, vacuum gage; 3, vacuum jar; 4, capillary probe; 5, photoelectric sensors; 6, electric circuit; 7, computer; 8, foam fractionation column; 9, foamate collector; 10, masterflex liquid pump; 11, feed reservoir; 12, compressed air; 13, humidifier; 14, air rotameter; 15, valve; 16, residue; 17, valve; 18, sparger.

Ovalbumin (Grade II, lot 88H1447) was purchased from Sigma (St. Louis, MO). An aqueous solution of ovalbumin was used in the foam fractionation experiments. The solution was prepared by dissolving a given amount of solid ovalbumin in water to give the desired concentration. Ovalbumin concentration was determined by the Coomassie Blue method *(10)*.

The bubble size distributions and ε_g at different positions (Fig. 2) of the foam fractionation column (the so-called point values) were measured using a photoelectric capillary probe, which was previously described *(11)*.

Table 1 gives the chosen ranges of the three experimental variables: feed ovalbumin concentration, superficial gas velocity, and feed flow rate. The pH of the feed solution was 6.5, which was the value without any pH adjustment.

Definitions

The Sauter mean diameter was defined as follows:

$$d_{32} = \frac{\sum_{i=1}^{N} d_i^3}{\sum_{i=1}^{N} d_i^2} \tag{1}$$

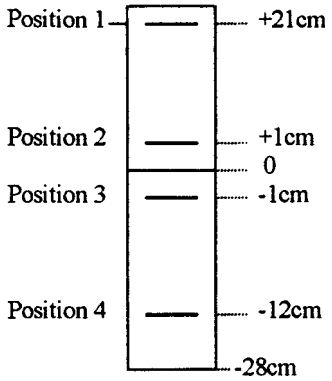

Fig. 2. Measurement points along column. The 0 mark represents the interface between the bulk liquid phase (at the bottom) and the foam phase (at the top) *(9)*.

Table 1
Experimental Operating Variables and Their Ranges

Ovalbumin concentration (mg/L)	Superficial gas velocity (cm/s)	Feed flow rate (mL/min)
30–100	0.05, 0.1, 0.2	24, 45, 60

Specific area *(9)* was defined as follows:

$$a = \frac{6\varepsilon_g}{d_{32}} \tag{2}$$

Local enrichment was defined as follows:

$$ER_l = \frac{C_{fl}}{C_0} \tag{3}$$

$d_i$and thus d_{32}, and ε_g were obtained from the online bubble size measurement directly. The local foamate concentration, C_{fl}, was obtained experimentally (as discussed in the previous section). It also was estimated using a local mass balance:

$$C_{fl} = (C_{ll}\varepsilon_l + \Gamma a)/\varepsilon_l \tag{4}$$

when we assume that the surface concentration of ovalbumin, Γ, was approximately the saturated surface concentration (since the liquid concentration used herein was above ovalbumin's critical micelle concentration, 20 mg/L at pH 6.5 *[9]*) which was estimated from the surface tension data *(9)*, with the measured ε_g and the calculated specific area (a) values, plus an assumed local liquid concentration, C_{ll}.

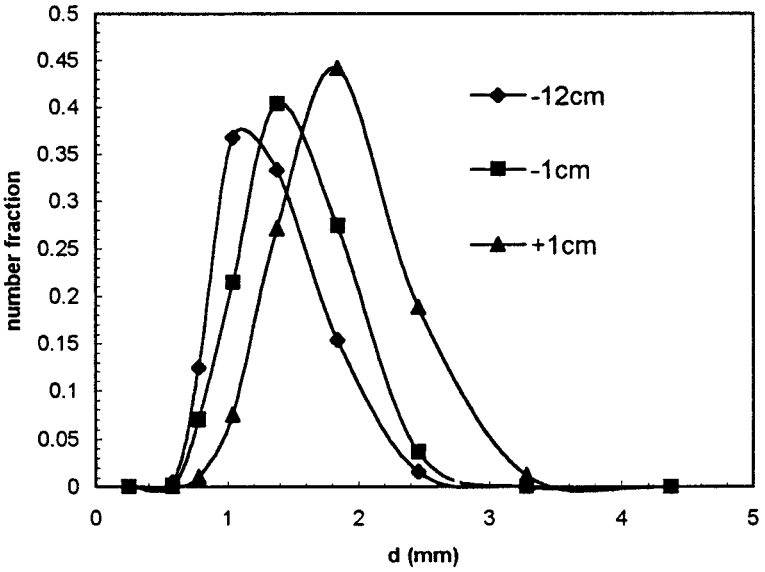

Fig. 3. Variation in bubble size distribution with position (at 3.5 min) at –12 cm, –1 cm, and +1 cm for superficial gas velocity of 0.05 cm/s, feed flow rate of 45 mL/min, feed concentration of 38 mg/L.

Results and Discussion

Bubble Size Distribution in Bulk Liquid and Lower Foam Phases

Figures 3 shows several typical bubble size distributions in the foam fractionation column. The bubble size (diameter) in the bulk liquid pool ranged from 0.6 to 2.5 mm, and, the bubble diameter in the lower foam phase had a wider range of 0.8 to 4.6 mm. Further investigation *(9)* indicated that the bubble size distributions shown here were closer to a log normal distribution than a normal distribution. Lage and Espósito *(12)*, Calvert and Nezhati *(13)*, and Wong et al. *(7)* also observed a log normal distribution of the bubble sizes in a bubble or a foam column (where bubbles are generated by sparging) using a two-dimensional photography method. The Sauter mean diameter, d_{32}, (obtained from Fig. 3) was 1.37, 1.52, and 2.1 mm for the –12, –1, and +1cm positions, respectively. The d_{32} values in the bulk liquid pool were quite close, exhibiting slight growth, which resulted from the decrease in static pressure corresponding to the reduction in the liquid level above the bubble. The larger and wider range of bubbles in the lower foam phase may have resulted from the enhanced bubble coalescence resulting from the closer distances between attaching bubbles as the liquid drained. For the position +21 cm, the bubble size distribution could not be obtained accurately with our measurements because either sufficient bubbles could not be sampled (number <10) at the tested lower suction speeds or the larger bubbles were strained inside the narrow capillary at the tested higher suction speeds. The breakage of

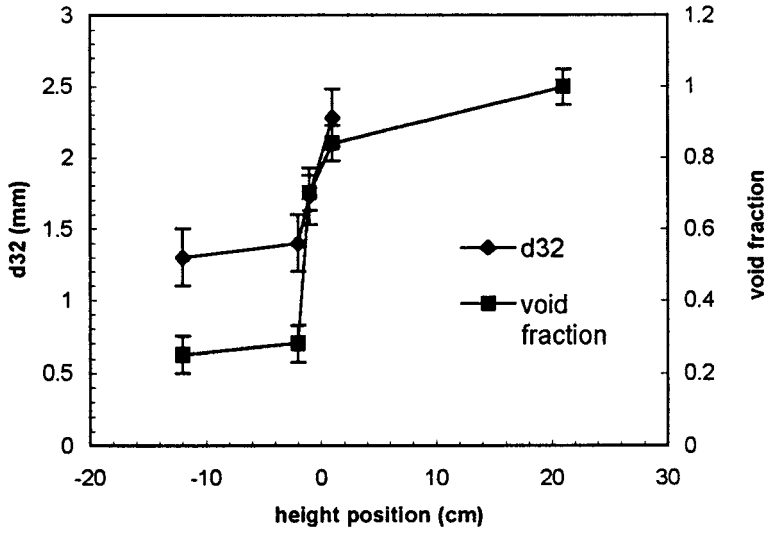

Fig. 4. Variation in d_{32} and ε_g with column position for superficial gas velocity of 0.1 cm/s, feed flow rate of 24 L/min, and feed concentration of 40 mg/L.

the larger bubble cells on entry into the capillary tube also made accurate measurements difficult *(9)* at the higher foam positions.

Variations in d_{32}, ε_g, a, *and* ER_l *with Column Position*

Figure 4 displays d_{32} and ε_g along the height of the foam fractionation column for a superficial gas velocity of 0.1 cm/s, a feed flow rate of 24 mL/min, and a feed concentration of 40 mg/L. One additional point at –2 cm was added to the three measurements of –12 cm, –1 cm and +1 cm to help delineate the transition of d_{32} around the bulk liquid-foam interface. In the bulk liquid pool, the bubble size and void fraction did not change significantly except at the column positions close to 0 cm (bulk liquid-foam interface), where they increased abruptly. The increase in bubble size can be explained as a result of bubble coalescence. The ε_g near the bulk liquid-foam interface, measured from 0.7 to 0.8, was close to 0.74, the theoretical value for closely packed spheres (here, bubbles). As bubbles left the bulk liquid-foam interface, strong gravity drainage caused a rapid increase in ε_g, as shown at position +1 cm ($\varepsilon_g > 0.8$).

Figure 5 shows that in the bulk liquid pool, the specific area, *a*, was small (about 12 cm^2/cm^3 under the given conditions) and did not increase greatly along the height of the column until the interface was approached. Since it has been shown in Fig. 4 that d_{32} and ε_g did not change significantly in the bulk liquid pool, this result (almost constant *a*) was expected. Near the bulk liquid-foam interface (–1 cm), *a* experienced a steep increase and doubled in value in the lower bulk liquid pool to about 25.0 cm^2/cm^3. This was owing to ε_g more than doubling coupled with a less than doubling in

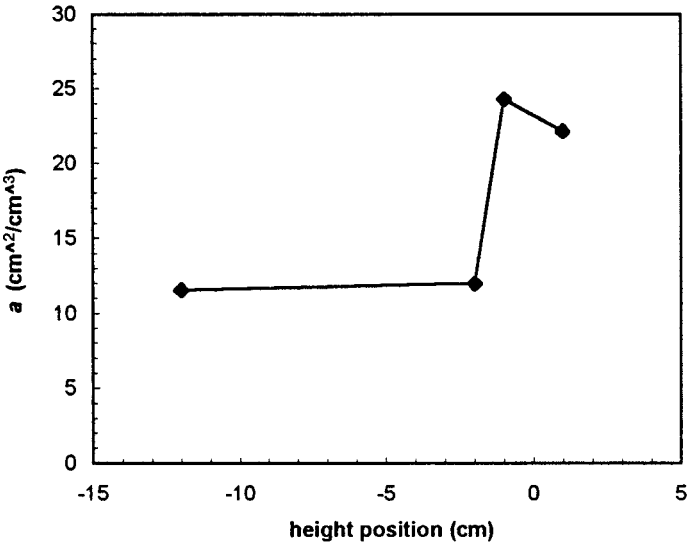

Fig. 5. Variation in a with foam fractionation column position for given superficial gas velocity of 0.1 cm/s, feed flow rate of 24 mL/min, and feed concentration of 40 mg/L.

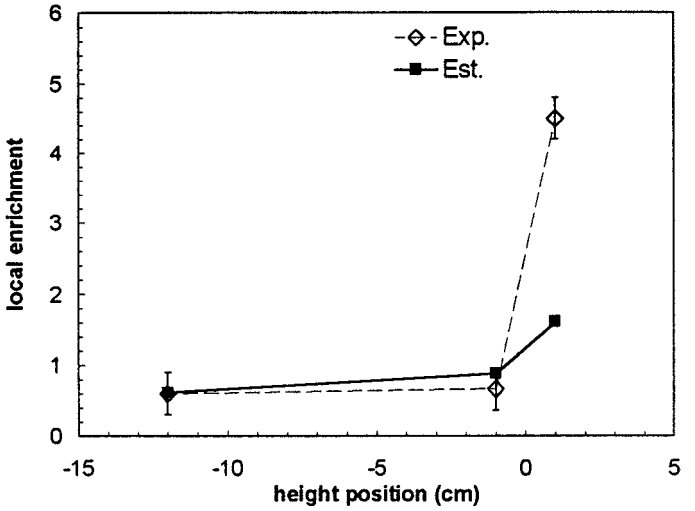

Fig. 6. Comparison between experimental ER_l and estimated ER_l for superficial gas velocity of 0.1 cm/s, feed flow rate of 24 mL/min, and feed concentration of about 36 mg/L.

d_{32} as the position changed from –2 cm to –1 cm. Interestingly, the specific area at +1 cm was a little smaller than that at –1 cm. The reason for this drop is that bubble coalescence in the foam phase (+1 cm) caused d_{32} to increase more than the void fraction.

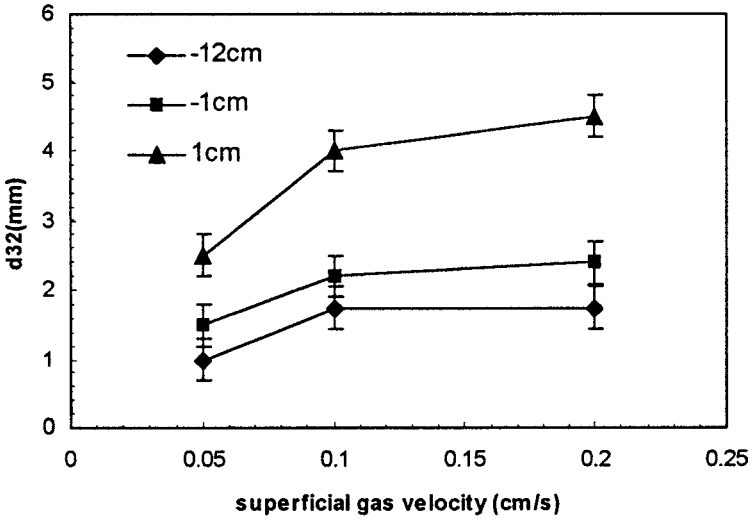

Fig. 7. Effect of superficial gas velocity on d_{32} for feed flow rate of 45 mL/min and feed concentration of 40 mg/L.

Figure 6 compares the estimated and the direct experimental local enrichment results. ER_l in the bulk liquid pool was <1, indicating that ovalbumin was depleted from the bulk liquid pool. ER_l in the lower foam phase was >1, indicating the ability of the foam phase to concentrate ovalbumin. It also shows that the estimated ER_l values for the two bulk liquid positions agreed with the experimental values. But for the lower foam phase the estimated ER_l (1.6) was much less than the experimental value (4.5). The underestimation in the lower foam phase may be the result of the fact that the assumed liquid concentration of the bulk liquid was lower than the actual value. Errors in the surface concentration and the ε_g could also cause the underestimation. The correlation between the a and the ER_l shows that the increased ER_l in the foam phase was the result of the increase in a, caused by drainage (shown by the abrupt increase in ε_g) when bubbles rose out of the bulk liquid pool.

Effect of Superficial Gas Velocity on d_{32}, ε_g, a, *and* ER_l

The effect of the superficial gas velocity on d_{32} is displayed in Fig. 7. As the superficial gas velocity increased, d_{32} increased in both the bulk liquid pool and the lower foam phase. The effect is more significant at lower superficial gas velocity values (from 0.05 to 0.1 cm/s). In particular, in the bulk liquid pool, d_{32} nearly leveled off when the superficial gas velocity was >0.1 cm/s. The results presented here are consistent with Wong et al.'s findings *(7)*. One possible reason for the increase in d_{32} is that as the superficial gas velocity increased, the bubble residence times in both the bulk liquid and the foam phase became shorter. The shorter residence time in the bulk liquid may cause incomplete adsorption of protein onto

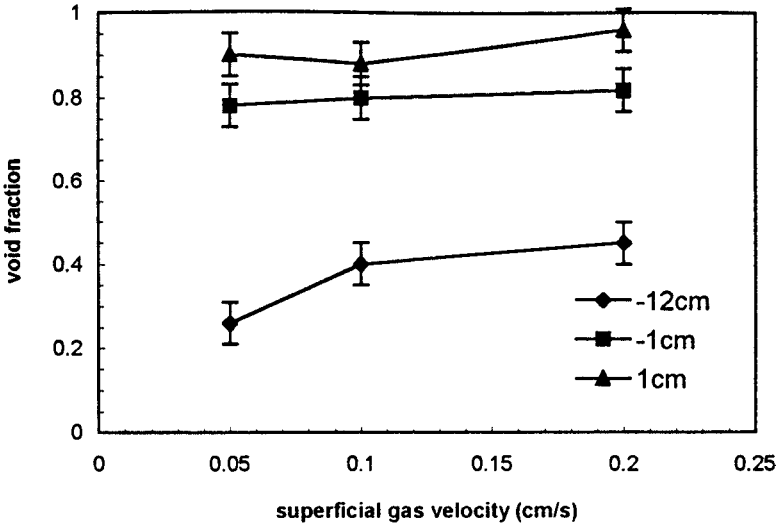

Fig. 8. Effect of superficial gas velocity on ε_g for feed flow rate of 24 mL/min and feed concentration of 40 mg/L.

the bubble surface. This, in turn, would cause a lower bubble surface concentration, which may contribute to a larger bubble size. Expansion of bubbles in the bulk liquid became less significant, owing to the shorter residence time. Therefore, for larger superficial gas velocities, the increase in bubble size became less significant in the bulk liquid phase. In the foam phase, coalescence was limited owing to the shorter residence times (larger superficial gas velocities), resulting in less of an increase in bubble size.

The ε_g was generally higher for a higher superficial gas velocity, as shown in Fig. 8. This effect was most significant for the case of –12 cm position. When the superficial gas velocity rose above 0.1 cm/s, the increase in ε_g at the –12-cm position became less significant. For the upper bulk liquid (–1 cm) and the lower foam phase (+1 cm), the ε_g was barely affected by changes in superficial gas velocity, since the ε_g was already close to that of closely packed spheres.

The variation in a with the superficial gas velocity is shown in Fig. 9. As the superficial gas velocity increased, a values for both –1 cm and +1 cm first decreased and then almost leveled off. For the lower bulk liquid position –12 cm, a almost remained constant for different superficial gas velocities.

Figure 10 displays the ER_l values in the upper bulk liquid pool (–1 cm) and lower foam phase (+1 cm) for different superficial gas velocities. The estimated ER_l values, at –1 cm, were larger than the experimental values by up to 50%. For the case of +1 cm, the estimated ER_l values were about 40% lower than the experimental values. The same general trend for the estimated and experimental enrichments as a function of the superficial gas velocity was maintained for the –1 cm case. The ER_l experimental value decreased as the superficial gas velocity increased and that decrease

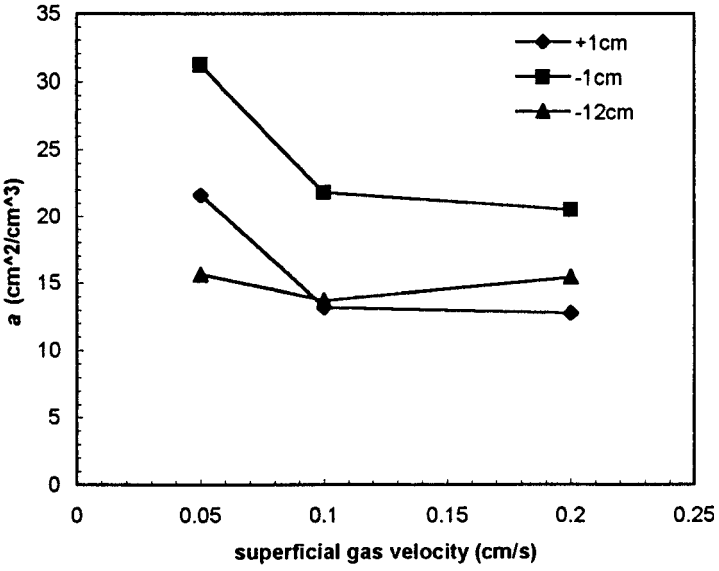

Fig. 9. Effect of the superficial gas velocity on *a* for feed flow rate of 24 mL/min and feed concentration of 40 mg/L.

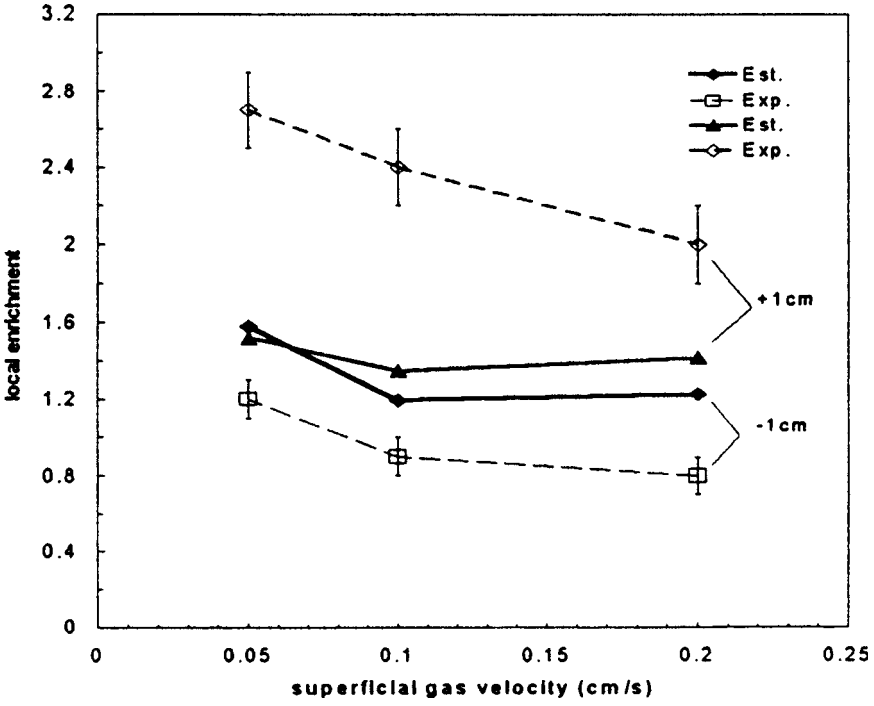

Fig. 10. Comparison between estimated and experimental ER_l values in upper bulk liquid phase (–1 cm) and lower foam phase (+1 cm) for different superficial gas velocities, feed flow rate of 45 mL/min, and feed concentration of 40 mg/L.

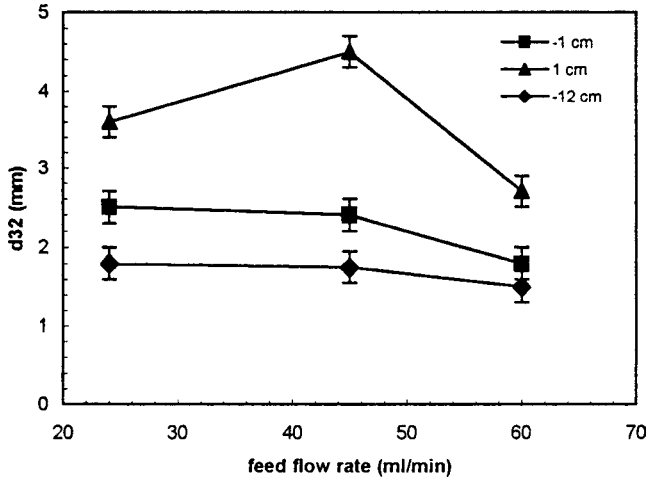

Fig. 11. Effect of feed flow rate on d_{32} at different positions for superficial gas velocity of 0.1 cm/s, and feed concentration of 40 mg/L.

became less significant at higher superficial gas velocities. This change was similar to the corresponding change in *a* shown in Fig. 9, where *a* became smaller as the superficial gas velocity was increased. Therefore, *a* of the bubbles was correlated with the enrichment, and because of the enhanced protein-holding ability of the larger area, it played an important role in obtaining high ER_l values in a foam fractionation column, especially for the lower foam phase.

Effect of Feed Flow Rate on d_{32}, ε_g, a, *and* ER_l

Figure 11 shows the variation in d_{32} with the feed flow rate for all the three positions measured (–12 cm, –1 cm, and +1 cm). It appeared that the feed flow rate had a more significant effect on the d_{32} in the lower foam phase than in the bulk liquid pool. This followed because the bubble coalescence that occurred in the foam phase was more sensitive to the bubble surface concentration, and, thus, the bulk liquid concentration, which was higher for larger feed flow rates. For the lower foam phase, when the feed flow rate was at the intermediate value, 45 mL/min, d_{32} was the largest. When the feed flow rate increased above 45 mL/min, d_{32} decreased owing to the higher bulk liquid concentration, which resulted from the larger feed flow rate.

The feed flow rate was found to affect the ε_g in both the bulk liquid and the foam phases, as shown in Fig. 12. In the lower foam phase, the ε_g increased as feed flow rate increased. In the upper bulk liquid phase, ε_g first increased with an increase in the feed flow rate and then leveled off to a constant value.

Similar data on bubble size and ε_g values for different feed flow rates in a foam fractionation column, for comparision, have not been found in the

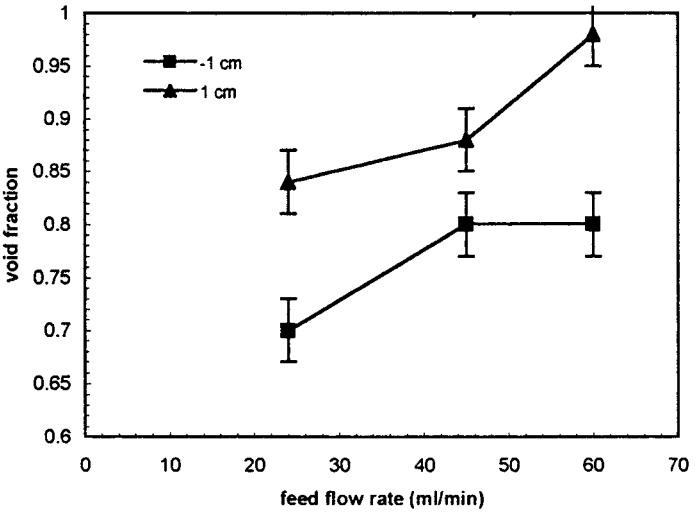

Fig. 12. Effect of feed flow rate on ε_g near bulk liquid-foam interface for superficial gas velocity of 0.1 cm/s and feed concentration of 40 mg/L.

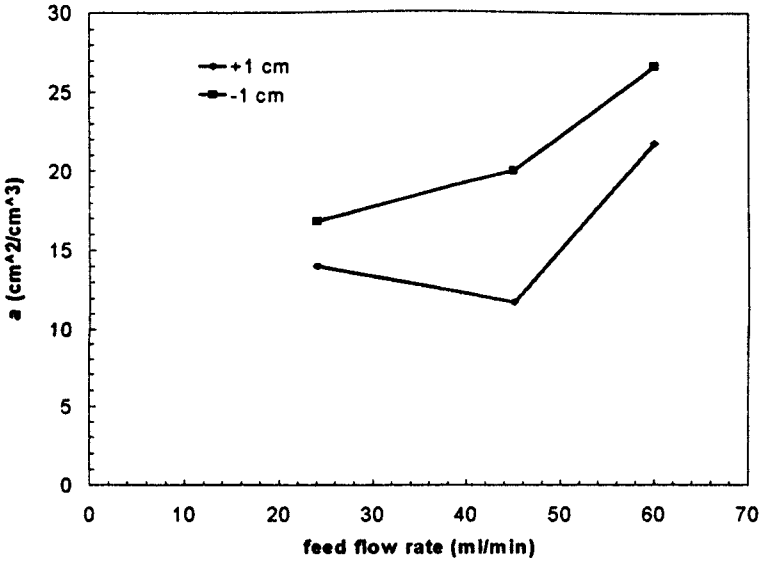

Fig. 13. Effect of feed flow rate on *a* for superficial gas velocity of 0.1 cm/s, feed concentration of 40 mg/L, and pH 6.5.

literature, presumably because of the difficulty in obtaining local bubble size distributions and ε_g values in a foam fractionation column *(13)*. The photoelectric capillary method developed in the present study was easy to use and rapid. It can easily provide bubble size and ε_g information in a foam column to help develop the basis for mechanisms of foam fractionation.

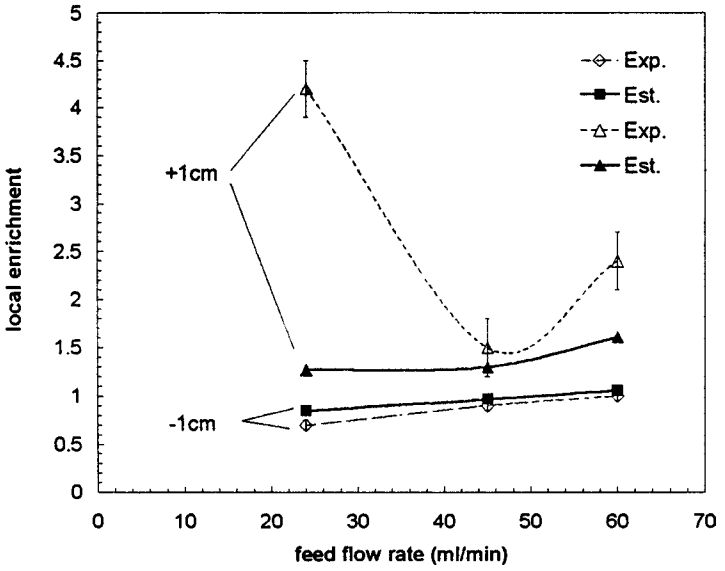

Fig. 14. Comparison between estimated ER_l values and experimental values in upper bulk liquid pool (–1 cm) and lower foam phase (+1 cm) for superficial gas velocity of 0.1 cm/s and feed concentration of 40 mg/L.

Figure 13 displays the effect of the feed flow rate on a. When the feed flow rate was increased, a was increased, which was the general trend for both the upper bulk liquid phase (–1 cm) and the lower foam phase (+1 cm). In the lower foam phase (+1 cm), for the intermediate feed flow rate of 45 mL/min, a dropped below that of the lowest flow rate, perhaps because of errors in the underlying ε_g or bubble size.

Figure 14 shows the ER_l values for different feed flow rates. The ER_l values were overestimated about 20% for the –1 cm case. With the increase in the feed flow rate, the ER_l at –1 cm increased because the increased feed flow rate caused the bulk liquid concentration to increase. On the other hand, a in the upper bulk liquid phase became larger when the feed flow rate increased, which also contributed to the increase in the ER_l. For the +1 cm case, the ER_l was underestimated, perhaps because the assumed liquid concentration (set equal to the feed concentration) was lower than the actual value. The estimated ER_l at the intermediate feed flow rate was very close to the experimental value, but for either lower or higher feed flow rates, the estimated values were much smaller than the experimental values (about 33 and 70%, respectively). Compared with the results on a in the lower foam phase (+1 cm) for different feed flow rates (Fig. 13), the estimated ER_l seemed reasonable. At the highest feed flow rate, the higher ε_g and the larger a resulted in a higher ER_l than the intermediate feed f low rate. Still, the assumption of lower liquid concentration in the lower foam phase than the actual value may cause the surface term (Γa) in Eq. 4 to dominate, which, in turn, would lead to the underestimated ER_l values

exhibited in Fig. 14. The reason for the highest experimental ER_l at the lowest feed flow rate is not clear.

Conclusion

From the measurements of bubble size in the continuous foam fractionation of ovalbumin experiments, we determined that the bubble diameters at the two bulk liquid positions (–12 and –1 cm) were in the range of 0.5–3.0 mm, while the bubble diameter at the lower foam position (+1 cm) varied between 1.0 to 4.5 mm. Therefore, the bubble size distributions along the height of the column showed a shift toward large diameters and became even wider in the lower foam phase, indicating that bubble coalescence occurs throughout the column. d_{32} increased along the height of the foam fractionation column. This increase was more significant in the foam phase.

ε_g increased rapidly near the bulk liquid-foam interface but changed gradually in both the bulk liquid and foam phase. The void fraction values at positions –1 cm and +1 cm were close to 0.74, which is the theoretical value for the closely packed spheres. In the foam phase, ε_g reached values >90%.

a was small (about 12 cm^2/cm^3) and changed negligibly with the height of the column in the bulk liquid pool. At the bulk liquid-foam interface, a doubled abruptly so that in the lower foam phase its value was about 25.0 cm^2/cm^3.

The ER_l values in the bulk liquid phase were generally <1.0, being between 0.6 and 0.8, which reflected the depletion of ovalbumin from the bulk liquid pool. ER_l did not change greatly along the height of the column in the bulk liquid pool, indicating good mixing in the bulk liquid pool. ER_l in the lower foam phase was >1.0 and in the range of 1.1–7.5.

The correlation between a and ER_l showed that the increased ER_l in the foam phase was the result of the increase in a, which was caused by drainage (shown by the abrupt increase in ε_g) when bubbles rose out of the bulk liquid pool. Therefore, the bubble value of a played an important role in obtaining high ER_l values in a foam fractionation column, especially for the lower foam phase.

d_{32} in both the bulk liquid pool and the lower foam phase first increased as the superficial gas velocity increased, probably resulting from the reduced bubble residence time, which resulted in incomplete adsorption of ovalbumin and, thus, lower surface concentration. The increase in d_{32} was less significant when the superficial gas velocity rose above 0.1 cm/s.

In the lower foam phase, ε_g increased slightly as the superficial gas velocity increased, since it was always close to 0.74, the maximum value for closely packed spheres. For the lower bulk liquid phase, however, ε_g increased as the superficial gas velocity increased.

The estimated a became smaller for higher superficial gas velocities at a given column position owing to the increase in bubble size. ER_l in both

the bulk liquid and lower foam phases decreased when the superficial gas velocity increased. This correlation implied that the larger a of the bubbles is important for developing the higher enrichment.

The effect of the feed flow rate on bubble size, ε_g, a of the bubbles and, thus, ER_l is complex. The findings presented here are new and have not been previously reported in the literature.

When the feed flow rate changed from 25 to 60 mL/min, d_{32}, in the lower foam phase was more significantly affected than d_{32} in the bulk liquid pool. For the feed flow rate, 45 mL/min, d_{32}, was the largest in the lower foam phase. ε_g in the lower foam phase increased as the feed flow rate increased. For the two bulk liquid positions (–12 cm and –1 cm), d_{32} showed a gradual decrease as the feed flow rate increased from 25 to 60 mL/min. The calculated a increased as the feed flow rate increased in the upper bulk liquid and the lower foam phase.

The ER_l in the upper bulk liquid pool increased as the feed flow rate increased, since the bulk liquid concentration was raised as the feed flow rate increased. In the lower foam phase, ER_l was highest for the lowest feed flow rate and lowest for the intermediate feed flow rate. At the highest feed flow rate, the higher ε_g and the larger a resulted in a higher ER_l than at the intermediate feed flow rate.

Nomenclature

a = Specific area (cm^2 interfacial area/cm^3 column volume)
C_0 = Feed ovalbumin concentration (mg/L)
C_{fl} = Local foamate (collected in vacuum jar) concentration (mg/L)
C_{ll} = Local liquid concentration (mg/L)
d_{32} = Sauter mean diameter (mm)
d_i = Individual bubble diameter (mm)
ER_l = Local enrichment ratio
N = Total number of bubbles sampled
ε_l = Liquid holdup
ε_g = Void fraction
Γ = Surface concentration (mg/cm^2)

Acknowledgment

We are grateful to Yuqing Ding, a graduate student of Chemical Engineering Department at Vanderbilt University, for his help in suggesting and designing the photoelectric capillary probe. We also greatly appreciate financial support from the National Science Foundation (NSF No. CTS-9712846).

References

1. Rand, P. B. and Kraynik, A. M. (1983), *Soc. Petrol. Eng. J.* **23(1),** 152–254.
2. Sarma, S. R. and Khilar, K. C. (1988), *Ind. Eng. Chem. Res.* **27(5),** 892–894.

3. Bhattacharya, P., Ghosal, S. K., and Sen, K. (1991), *Separat. Sci. Technol.* **26(10/11),** 1279–1293.
4. Brown, A. K., Kaul, A., and Varley, J. (1999), *Biotechnol. Bioeng.* **62(3),** 278–290.
5. Brown, L., Narsimhan, G., and Wankat, P.C. (1990), *Biotechnol. Bioeng.* **36,** 947–959.
6. Uraizee, F. and Narsimhan, G. (1996), *Biotechnol. Bioeng.* **51,** 384–398.
7. Wong, C. H., Hossain, M. D., and Davies, C.E. (1996), *Bioprocess and Biosystems Engineering* **24,** 73–81.
8. Magrabi, S. A., Dlugogorski, B. Z., and Jameson, G. J. (1999), *Chem. Eng. Sci.* **54,** 4007–4022.
9. Du, L. (2001), PhD thesis, Vanderbilt University, Nashville, TN.
10. Bradford, M. M. (1976), *Anal. Biochem.* **72,** 248–254.
11. Du, L., Ding, Y., Prokop, A., and Tanner, R. D. (2001), *Appl. Biotechnol. Bioeng.* **91–93,** 387–404.
12. Lage, P. L. C. and Espósito, R. O. (1999), *Powder Technol.* **101,** 142–150.
13. Calvert, J. R. and Nezhati, K. (1987), *Int. J. Heat Fluid Flow* **8(2),** 102–106.